Chemical Science

ROYAL SOCIETY OF CHEMISTRY

EDGE ARTICLE

View Article Online
View Journal | View Issue



Cite this: *Chem. Sci.*, 2026, **17**, 5934

All publication charges for this article have been paid for by the Royal Society of Chemistry

# Luminescent core-isolated solvent-free liquids as a soft material platform for optical gas sensing

Shinsuke Ishihara, †*[a] Avijit Ghosh, †[ab] Tatsuya Mori,‡[a] Mandeep K. Chahal,[ac] Daniel T. Payne, [ad] Akinori Saeki, [e] Tsuyoshi Hyakutake[f] and Takashi Nakanishi *[a]

Received 30th October 2025
Accepted 21st January 2026

DOI: 10.1039/d5sc08398b

rsc.li/chemical-science

Solvent-free functional molecular liquids have attracted great interest as a new class of stimuli-responsive soft materials, yet their potential as optical gas sensors remains unexplored. Conventionally, luminescent organic molecules are employed in combination with a solid support or matrix. However, their performance in chemical sensing and optoelectronic devices is often hindered by adverse phenomena such as aggregation, concentration quenching, and photodegradation. In this study, we employ a strategy to isolate and wrap a phosphorescent Pt(II)-porphyrin core with bulky yet flexible branched alkyl chains, resulting in a solvent-free liquid at room temperature that demonstrates excellent properties for sensing oxygen ($O_2$) gas. Compared to reference material composed of Pt(II)-tetraphenylporphyrin and a highly gas-permeable polymer matrix, our Pt(II)-porphyrin liquid shows comparable sensitivity ($I_0/I_{100} = 75 \sim 90$), better linearity, and greater photostability in its $O_2$-responsive phosphorescence. This is attributed to the high homogeneity and gas solubility of the liquids, as well as to the shielding of luminescent-core units by bulky alkyl chains. The liquid nature of the materials allows for ratiometric sensing, where the compatibility of a phosphorescent Pt(II)-porphyrin liquid ($O_2$-sensitive) and a fluorescent alkyl-pyrene liquid ($O_2$-insensitive) enables reproducible monitoring of $O_2$ concentration without specific calibration. Indeed, these results highlight the significant benefits of core-isolated luminescent liquids in diverse sensing applications.



## Introduction

Functional molecular liquids (FMLs) have recently become a transformative category in soft functional materials.[1] Within this group, alkyl-π liquids—solvent-free systems with π-conjugated molecular units isolated and wrapped by bulky yet flexible branched alkyl chains—provide tunable optoelectronic properties and liquid-phase behaviors that differ from traditional solid-state frameworks.[2–4] These alkyl-π liquids have unique physical properties: molecular uniformity, fluidity, deformability, miscibility, and guest solubility, *etc.* Owing to their abundant designability for functional core units, various types of FMLs have been developed to date (*e.g.*, tunable luminescence including phosphorescence,[5–9] triplet-mediated photochemical functions,[10,11] optoelectronic- and energy-related functions,[12–14] permanent porosity and gas adsorption,[15,16] and guest- and mechano-responsiveness[17–21]). Among those intriguing FMLs, although alkyl-π liquids have been developed as stimuli-responsive liquid materials, to the best of our knowledge, no reports have demonstrated the utility of their liquid properties for optical gas sensing. In related works, Isoda *et al.* reported alkylated *N*-heteroacene liquids that change their fluorescence color upon exposure to HCl vapor, where the vapor responsiveness is accompanied by protonation-induced solidification of the liquids.[20,21] Unique aspects of alkyl-π liquids include their ability to provide a distinct mode of operation as stable liquid media that retain responsiveness and miscibility. According to Henry's law, the dissolution of gas molecules into liquids is proportional to their partial pressure.[22] This motivated us to elucidate the potential of alkyl-π luminescent liquids as optical gas sensors and unveil any fundamental

[a]*Research Center for Materials Nanoarchitectonics (MANA), National Institute for Materials Science (NIMS), 1-1 Namiki, Tsukuba, Ibaraki 305-0044, Japan. E-mail: ISHIHARA.Shinsuke@nims.go.jp; NAKANISHI.Takashi@nims.go.jp*

[b]*School of Applied Science & Technology, Department of Forensic Science & Technology, Maulana Abul Kalam Azad University of Technology, Haringhata 741249, West Bengal, India*

[c]*School of Chemistry and Forensic Science, University of Kent, Canterbury, CT2 7NH, UK*

[d]*School of Life, Health & Chemical Sciences, The Open University, Milton Keynes, MK7 6AA, UK*

[e]*Department of Applied Chemistry, Graduate School of Engineering, Osaka University, 2-1 Yamadaoka, Suita, Osaka, 565-0871, Japan*

[f]*Innovative Materials and Resources Research Center, Public Works Research Institute, 1-6 Minamihara, Tsukuba, Ibaraki, 305-8516, Japan*

† These authors contributed equally to this work.

‡ Present address: Department of Chemistry, Graduate School of Science and Integrated Research Consortium on Chemical Sciences (IRCCS), Nagoya University, Furo, Chikusa, Nagoya, 464-8602, Japan.

aspects distinct from conventional solid support or matrix systems.

Luminescent organic molecules (LOMs) have been utilized for optical sensing of physical, chemical, and biological events.[23–26] In particular, oxygen ($O_2$) is a vital target analyte[27–29] due to strong connections with the atmospheric environment, energy, and life, as exemplified by the spatiotemporal visualization of aerodynamics,[30] fuel cell operation,[31] and hypoxia in cancer cells.[32,33] Among the various optical detection modes (*e.g.*, wavelength, intensity, ratiometric, frequency, upconversion, lifetime, *etc.*), monitoring of luminescence intensity is widely utilized in $O_2$ sensing due to the low cost and simplicity of the devices.[24,29] Triplet photo-excited states of LOMs can be effectively quenched by $O_2$, which makes their phosphorescence intensity sensitive to $O_2$ levels. The interaction dynamics and correlation between luminescence intensity and a quencher's concentration are described by the Stern–Volmer equation (eqn (1)).[27]

$$I_0/I_x - 1 = K_{sv}[Q] \quad (1)$$

where $I_0$ and $I_x$ are, respectively, the emission intensity in the absence (0%) and the presence ($x$%) of a quencher (herein, $O_2$), and $K_{SV}$ is the Stern–Volmer constant.

Since the luminescence of LOMs is generally maximized in their discrete (*i.e.*, non-aggregated) states except for rare cases where molecular motion is restricted within the aggregate or confinement,[34] optical sensing is often performed in a solution (dissolved in water or organic solvent) or a composite with solid support or matrix (*e.g.*, polymers,[35–37] oxides,[38,39] porous materials,[40–42] and nanoparticles[43–45]). Consequently, the performance of optical $O_2$ sensors is influenced not only by LOMs but also by the compatibility and $O_2$ permeability of the solid support or matrix. Among various phosphorophores (*e.g.*, polycyclic aromatic carbons, transition metal complexes, and fullerenes), Pt(II) and Pd(II)-porphyrins are extensively studied for optical $O_2$ sensing because of their intense phosphorescence at room temperature.[27,46–48] For example, Amao *et al.* found that Pt(II)-octaethylporphyrin (**PtOEP**) embedded in a highly gas-permeable poly(1-trimethylsilyl-1-propyne) (**PTMSP**)[49] shows considerable sensitivity to $O_2$ ($I_0/I_{100} = 225$).[50] In contrast, the same Pt(II)-porphyrin embedded in polystyrene or poly-(dimethylsiloxane) exhibits only moderate sensitivity ($I_0/I_{100} = \sim 5$).

Here, we present the first demonstration of an optical oxygen ($O_2$) sensing based on a phosphorescent core-isolated solvent-free liquid, utilizing a Pt(II)-porphyrin core ([5,10,15,20-tetrakis(3,5-bis((2-hexyldecyl)oxy)phenyl)porphyrinato]platinum(II) **PtPL**, Fig. 1). The liquid exhibits benchmark-level sensitivity ($I_0/I_{100} = 75 \sim 90$), superior linearity, and improved photostability compared to conventional reference materials composed of Pt(II)-tetraphenylporphyrin (**PtTPP**)[51] and **PTMSP**. Additionally, by mixing **PtPL** with a fluorescent alkyl-pyrene liquid, we develop a robust ratiometric sensing that operates without specific calibration. This work provides novel insights into optical gas sensing, establishing luminescent solvent-free liquids not only as responsive FMLs but also as active media, opening a versatile pathway toward a future soft sensing platform.

## Results and discussion

To obtain Pt(II)-porphyrin liquid **PtPL**, a free-base liquid porphyrin with 2-hexyldecyl branched alkyl chains[13] was reacted

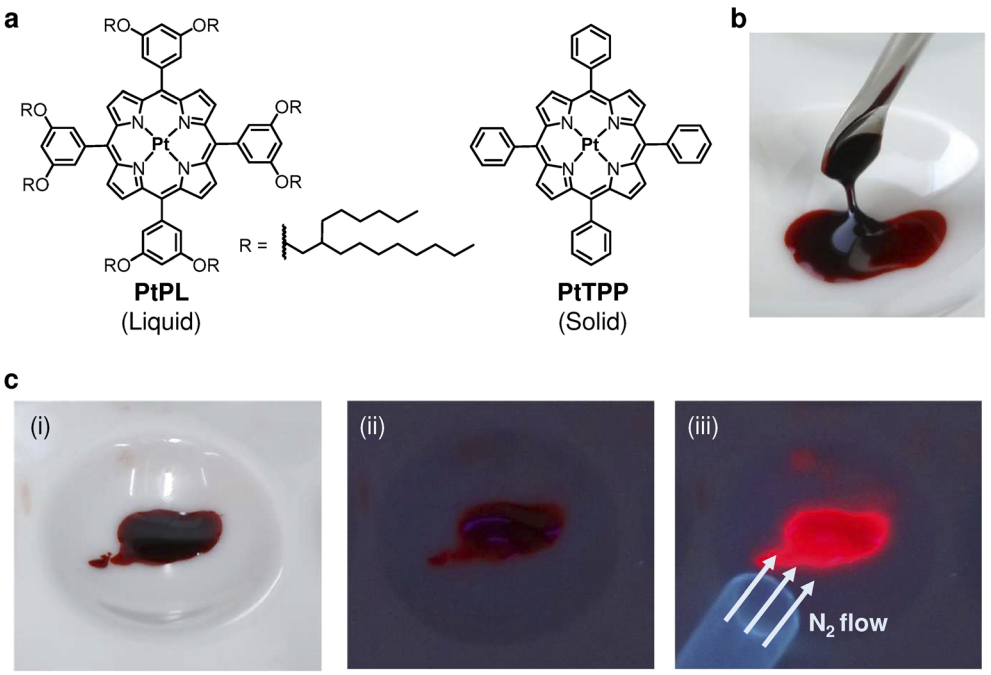


Fig. 1 (a) Chemical structures of Pt(II) porphyrins; alkylated liquid (**PtPL**) and solid **PtTPP** used in this study. (b) Photograph of **PtPL** at 20 °C showing solvent-free liquid appearance. (c) Phosphorescent property of **PtPL** observed under daylight in air (i), under UV light in air (ii), and under UV light with $N_2$ flow (iii).

with Pt(II)$Cl_2$ in refluxing benzonitrile for 4–5 h under argon (Ar) (Fig. 1a).[51] After purification and drying under vacuum, **PtPL** was obtained as a viscous red-orange liquid (Fig. 1b). Disappearance of the inner pyrrolic protons in the $^1$H NMR spectrum of **PtPL** indicates the successful insertion of a Pt(II) ion into the porphyrin core, and the high-resolution mass spectrum of **PtPL** is in agreement with its chemical formula, $[C_{172}H_{285}O_8N_4{}^{194}Pt]^+$ (Fig. S2–S5). Under ultraviolet (UV) irradiation, an intense red emission was observed from **PtPL** when under an $N_2$ or Ar atmosphere (Fig. 1c). The emission was largely quenched in air due to energy transfer from photo-excited **PtPL** to $O_2$. Thus, **PtPL** exhibits the expected phosphorescent properties for a long-lived triplet excited state. Even though branched alkyl chains surround the Pt(II) porphyrin core, small gas molecules can access the core through a mechanism akin to the facilitation of pyridine vapor into Zn(II) liquid porphyrin,[13] which is structurally similar to **PtPL** (see Fig. S6–9 and 21).

It is revealed that **PtPL** is a stable liquid at room temperature and shows optical properties in neat state almost identical to **PtTPP** in a diluted toluene solution (Fig. 2). A sample of **PtPL** sandwiched between glass plates is fluidic, and its cross-polarized optical microscopy (POM) image shows no birefringence, supporting the absence of long-range ordered domains (Fig. 2a). Differential scanning calorimetry (DSC) thermogram of **PtPL** shows only a reversible glass transition temperature ($T_g$) at around −40 °C; thus, **PtPL** maintains a liquid state above that temperature (Fig. 2b). Absorption and emission spectra of **PtPL** in neat liquid are similar to those of **PtPL** and **PtTPP** in toluene due to the bulky alkyl chains isolating the Pt(II)-porphyrin core from the surrounding environment (Fig. 2c and d). Note that the luminescent lifetime and quantum yield of **PtPL** were slightly longer and larger than those of **PtTPP** in toluene (Fig. S11 and Table S1).

As shown in Fig. 3a–c, the emission from neat film **PtPL** is quenched (signal intensity is reduced) as the concentration of $O_2$ in the atmosphere increases from 0% to 100%. There is a certain response to 0.03% $O_2$, and the emission intensity halved at an $O_2$ concentration of 1% (Fig. 3a). The Stern–Volmer plot of neat film **PtPL** shows linear correlations between $O_2$ concentration ($x$-axis) and $I_0/I_x - 1$ ($y$-axis). The value of $I_0/I_{100}$ is often used in the literature to represent $O_2$ sensitivity, and $I_0/I_{100} = \sim 90$ is much greater than most phosphorescent $O_2$ sensing materials ($I_0/I_{100} = 5 \sim 10$).[27,35,42] As described above, Amao *et al.* reported that **PtOEP** embedded in polystyrene or poly-(dimethylsiloxane) shows modest sensitivity ($I_0/I_{100} = \sim 5$).[50] Whereas, significant sensitivity to $O_2$ ($I_0/I_{100} = 225$) was obtained when **PtOEP** was embedded in a highly gas-permeable **PTMSP** polymer. Thus, our solvent-free liquid **PtPL** is a suitable medium for accommodating $O_2$ molecules from the gas phase. The higher sensitivity of Amao's film could be ascribed to

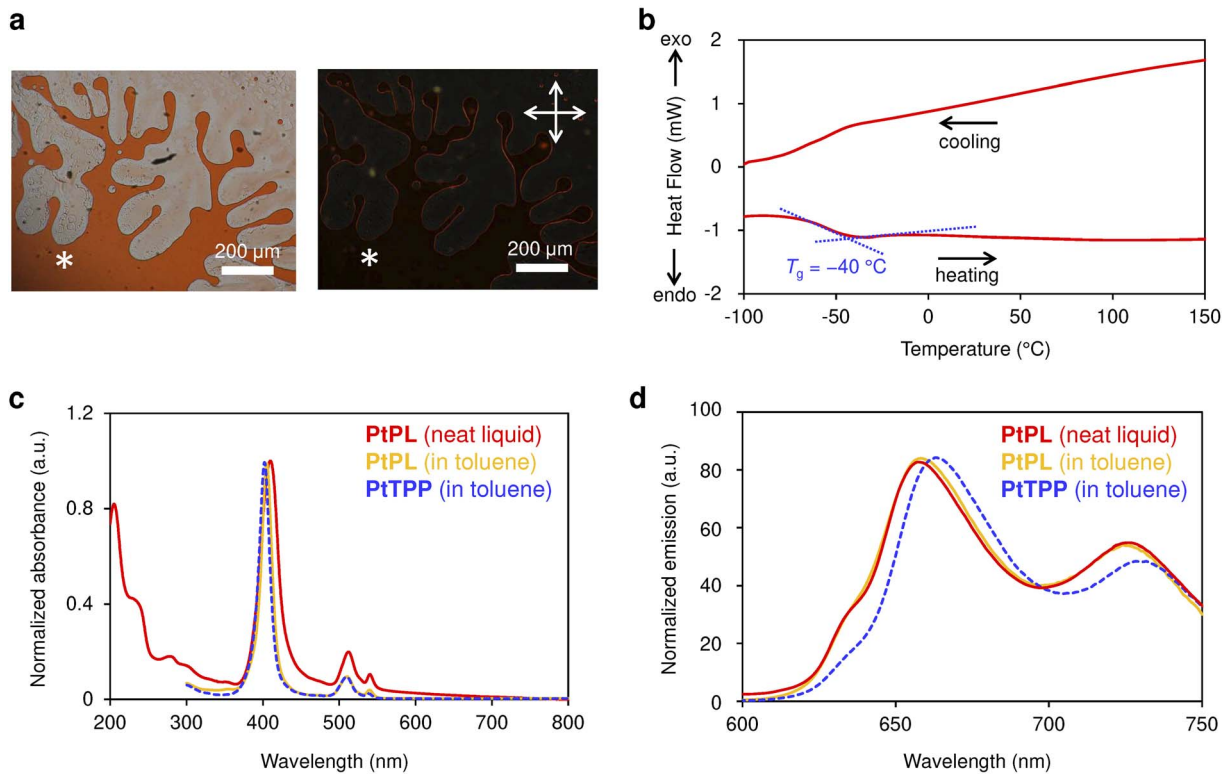


Fig. 2 (a) Optical microscopy images of **PtPL** sandwiched between glass plates without (left) and with (right) cross polarizers. Asterisks (*) represent the identical positions within the samples. (b) DSC thermogram in the 2nd heating and cooling trace of **PtPL** recorded under $N_2$ at a scan rate of 10 °C min$^{-1}$. (c) Absorption spectra of **PtPL** in neat liquid state. The absorption spectra of **PtPL** and **PtTPP** in toluene ($10^{-6}$ M) are shown for comparison. (d) Emission spectra of **PtPL** in neat liquid state ($\lambda_{ex} = 410$ nm) under argon (Ar). The emission spectra of **PtPL** and **PtTPP** in toluene ($10^{-6}$ M) under Ar are shown for comparison. Note that these emissions were largely quenched under air (see Fig. S12–14).

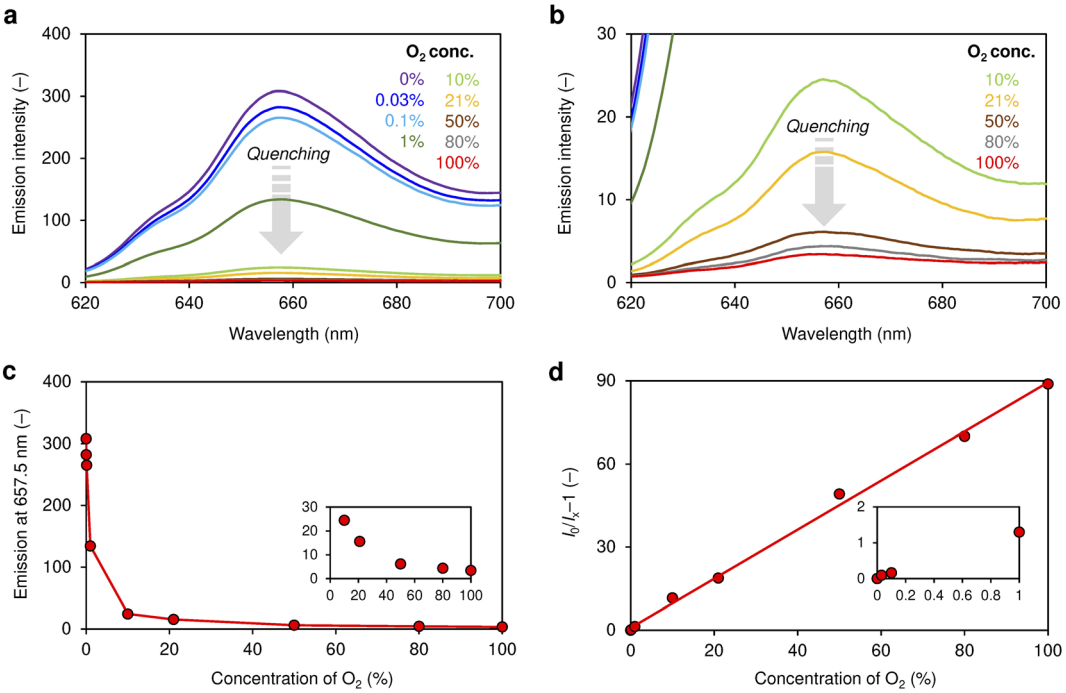


Fig. 3 (a and b) Emission spectra of a neat film **PtPL** ($\lambda_{ex}$ = 412 nm) measured under various $O_2$ concentrations (a; with higher emission intensities, b; emission intensities lower than 30). See Fig. S10 for photographs illustrating the emission changes of neat **PtPL** films at different $O_2$ levels. (c) Plot of $O_2$ concentration *vs.* emission intensity ($\lambda_{em}$ = 657.5 nm) in a neat film **PtPL**. Inset shows intensities lower than 30. (d) Stern–Volmer plot of a neat film **PtPL** ($\lambda_{em}$ = 657.5 nm) for $O_2$ sensing. Inset shows the plot for lower $O_2$ concentration than 1%. It is worth noting that the phosphorescence of **PtPL** shows little sensitivity to humidity, whereas it is sensitive to temperature and air pressure (see Fig. S15–17).

the excellent gas permeability of **PTMSP** as well as minimum substituents around the Pt(II)-porphyrin unit, enabling efficient energy transfer to proximal $O_2$. However, it should be noted that the porphyrin concentration in the Amao's film was very dilute (*ca.* $2.9 \times 10^{-5}$ mol dm$^{-3}$, estimated as *ca.* 0.003 wt% based on molecular weight of the **PtOEP** (727.8 g mol$^{-1}$) and density of **PTMSP** (0.7 g cm$^{-3}$)[52]), presumably for preventing undesirable aggregation of porphyrins in the polymer matrix. Therefore, compared to the neat liquid **PtPL**, the brightness of the **PtOEP–PTMSP** film should be modest.

To investigate the effect of the bulky alkyl side chains compared to a porous polymer matrix, the $O_2$ sensing performance of the neat liquid **PtPL** was compared with **PtTPP–PTMSP** and **PtPL–PTMSP** composites. A solution of **PtTPP** and **PTMSP** was spin-coated on a quartz substrate, and the optical properties of the thin films were investigated (Fig. 4a). Absorption signals corresponding to the Soret-band ($\lambda_{max}$ = 401 nm) of **PtTPP** linearly increased when the amount of **PtTPP** was increased from 0.2 to 20 wt% (Fig. 4b). However, the absorption signals did not grow beyond 20 wt%, suggesting aggregation or precipitation of **PtTPP** either within or outside the polymer matrix. In contrast, absorption signals of **PtPL** blended into **PTMSP** ($\lambda_{max}$ = 406 nm) did not saturate even at 80 wt% owing to the absence of aggregation of **PtPL** in the **PtPL–PTMSP** composite (Fig. 4c). Composite films of **PtTPP–PTMSP** (1, 5, 20, and 50 wt%) exhibited slightly better sensitivity to $O_2$ ($I_0/I_{100}$ = ~120) than a neat liquid film of **PtPL** ($I_0/I_{100}$ = ~90), which can be attributed to the higher gas permeability of **PTMSP** compared to **PtPL** (Fig. 4d). The linearity of each plot was quantitatively assessed using the coefficient of determination ($R^2$) obtained from linear fitting, showing moderate linearity ($R^2$ = 0.84–0.97). In contrast, **PtPL–PTMSP** displays clear composition-dependent behavior (Fig. 4e). At low loadings (1, 5, and 20 wt%), a nonlinear response with high sensitivity is observed. This high sensitivity can be attributed to the high gas permeability of the **PTMSP** matrix as well as the increased number of $O_2$ molecules available per **PtPL** molecule. Another possible interpretation is that **PtPL**, bearing branched alkyl chains reminiscent of those typically present in plasticizers, may slightly modify the local polymer environment, potentially facilitating $O_2$ diffusion. By contrast, at higher loadings (50 and 100 wt%), the Stern–Volmer plots exhibit excellent linearity ($R^2$ > 0.99), while maintaining a sufficiently high level of sensitivity compared with other materials, despite some reduction. Such excellent linearity is advantageous for the quantification of a wide $O_2$ range based on two-point calibration. Downward-curved Stern–Volmer plots are commonly observed in sensor films and are often attributed to the presence of multiple emissive states with different luminescence lifetimes and/or quenching efficiencies within heterogeneous matrices.[27,53–56] Thus, the improvement of linearity is likely due to the increased homogeneity of the sensing phase upon reducing the influence of the polymer matrix, which suppresses microenvironmental heterogeneity. Although neat liquid **PtPL** shows the lowest sensitivity among the samples in Fig. 4e, this limitation is addressed in the blended liquid system discussed in a later

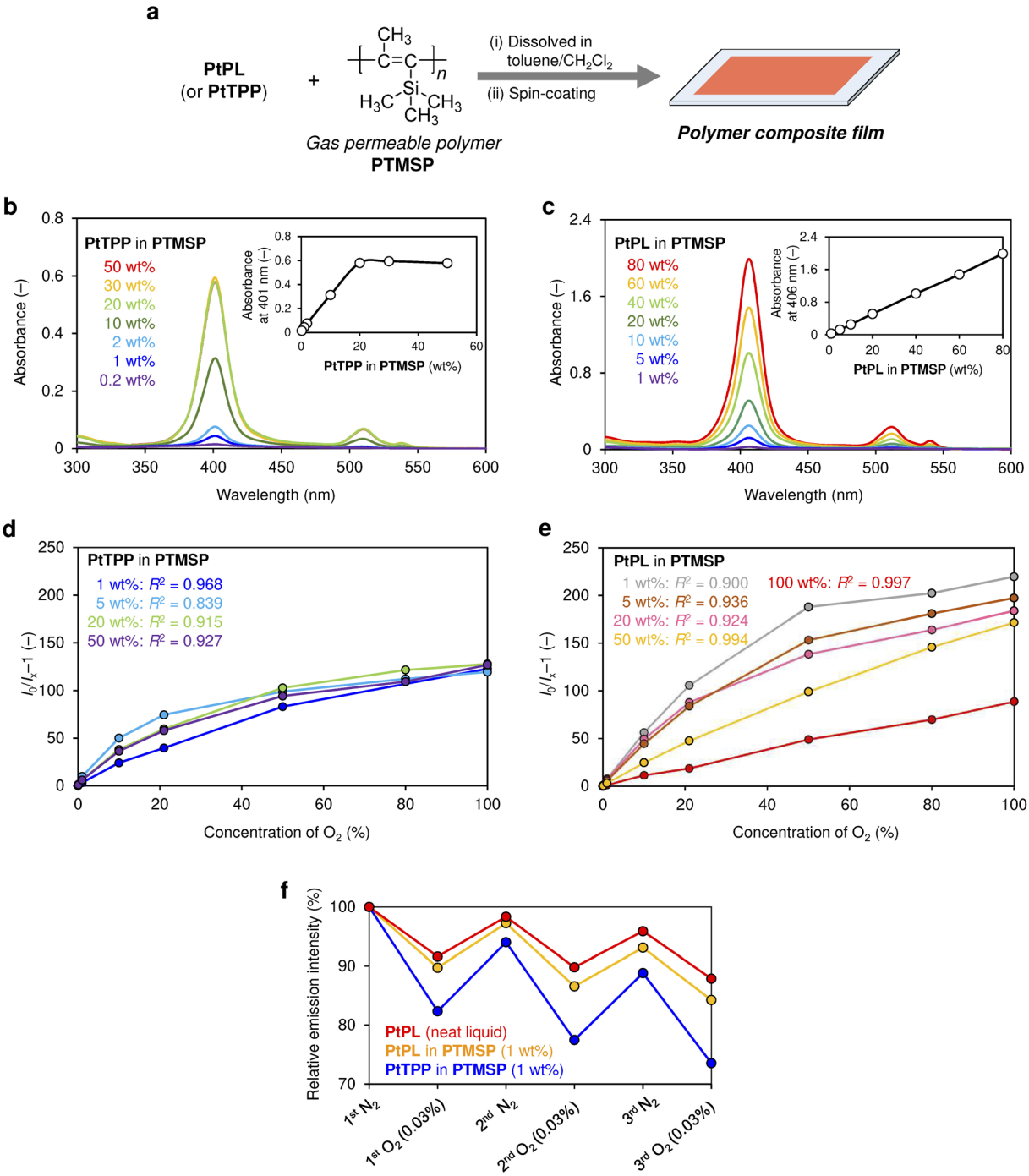


Fig. 4 (a) Preparation of polymer composite films. (b) Absorption spectra of **PtTPP–PTMSP** composite film with various amounts of **PtTPP**. (c) Absorption spectra of **PtPL–PTMSP** composite film with various amounts of **PtPL**. (d) Stern–Volmer plots of **PtTPP–PTMSP** composite films (1, 5, 20, and 50 wt%). $R^2$ denotes the coefficient of determination for the linear fit. (e) Stern–Volmer plots of neat liquid **PtPL** (100 wt%) and **PtPL–PTMSP** composite films (1, 5, 20, and 50 wt%). (f) Decay of emission intensity upon repeated exposure to excited beam irradiations under $N_2$ and 0.03% $O_2$.

section, where both high sensitivity and good linearity are simultaneously achieved.

Notably, neat liquid **PtPL** shows better photostability than **PtTPP–PTMSP** upon repeated measurements, which can be ascribed to protecting the Pt(II)-porphyrin unit by the bulky alkyl chains (Fig. 4f). Although fluorinated porphyrins are known to show improved photostability,[57] fluorinated organic compounds potentially cause environmental concerns due to poor biodegradability. The core-shielding effect of phosphorescent liquids (*e.g.*, **PtPL**) by hydrocarbon alkyl chains is advantageous in this regard. Toward practical implementation, photostability could be further improved by elongating or

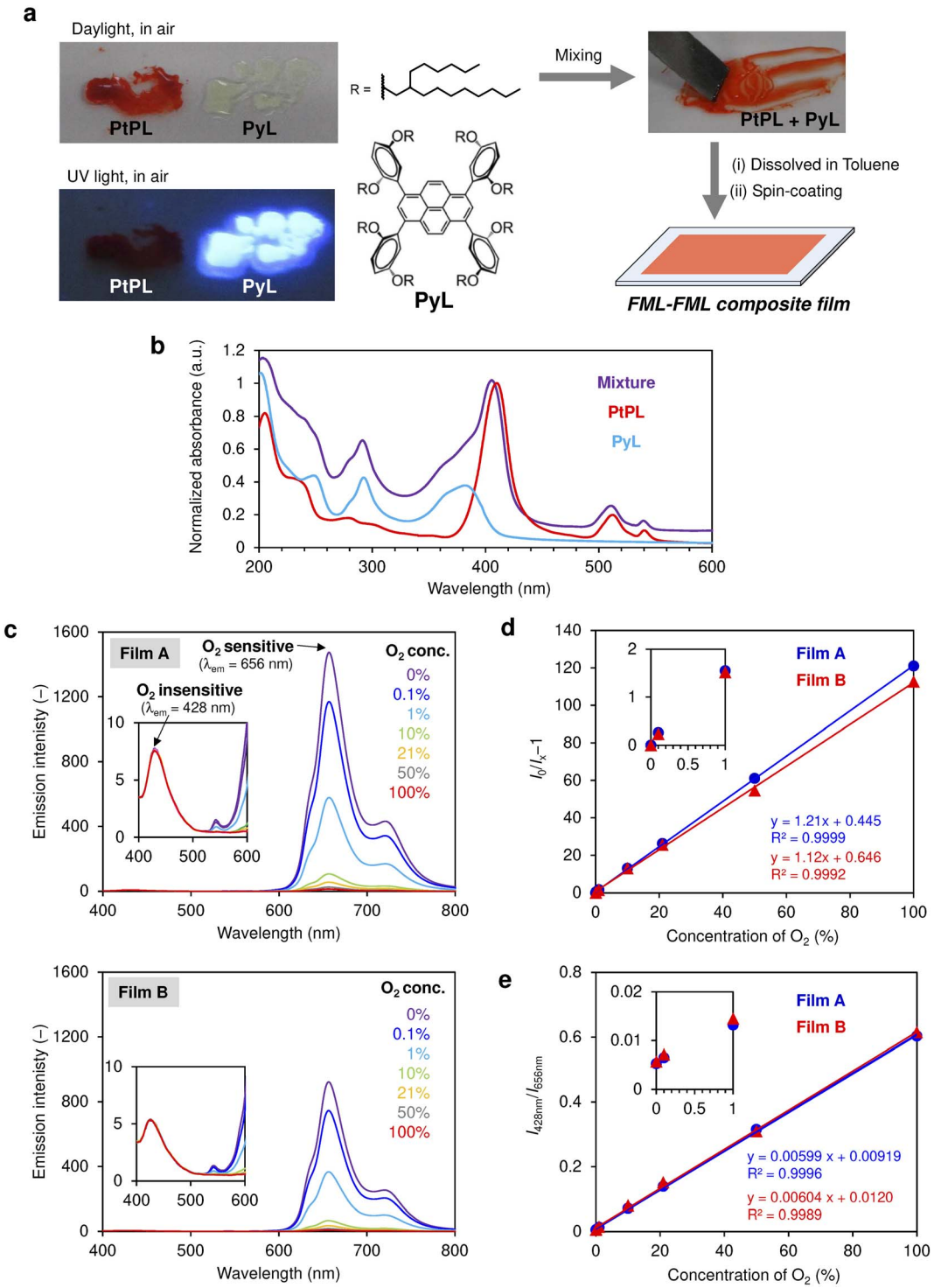


Fig. 5 (a) Blending of phosphorescent liquid **PtPL** and fluorescent liquid **PyL**. (b) Absorption spectrum of the mixed liquid film of **PtPL+PyL** (1 : 2, by weight) measured in air. For comparison, the absorption spectra of the individual neat liquids (**PtPL** and **PyL**), measured separately, are also shown. (c) Emission spectra ($\lambda_{ex}$ = 360 nm) of the mixed liquid film of **PtPL+PyL** (1 : 2, by weight) under various $O_2$ levels. The excitation wavelength was selected to simultaneously excite both **PtPL** and **PyL** while minimizing photobleaching caused by shorter-wavelength UV irradiation. Based on emission intensity, film A has approximately double the loading of liquids compared to film B. (d) Stern–Volmer plots obtained from phosphorescence ($\lambda_{em}$ = 656 nm) of films A and B. (e) Ratiometric plots obtained from $O_2$-insensitive fluorescence ($\lambda_{em}$ = 428 nm) and $O_2$-sensitive phosphorescence ($\lambda_{em}$ = 656 nm) of films A and B.

densifying the branched alkyl chains; however, this may adversely affect $O_2$ sensitivity because of reduced energy transfer efficiency. Therefore, photostability and sensitivity should be balanced depending on the aim of the application. We note that the present study focused on the equilibrium response to $O_2$, and response time was not evaluated due to the

unavailability of appropriate equipment. Overall, these studies elucidated, for the first time, that phosphorescent solvent-free liquids can be a promising platform for creating advanced optical gas sensors with high dye-loading amounts, excellent sensitivity, linearity, and photostability.

Finally, ratiometric optical $O_2$ sensing was performed simply by blending **PtPL** with an alkylated pyrene fluorescent ($O_2$-insensitive) liquid **PyL**[58] (Fig. 5a and S18). The emission intensity of dye-loaded polymeric films can be influenced by various factors such as beam intensity, film thickness, and homogeneity of LOMs in the polymer matrix, and the accurate determination of $I_0$ (*i.e.*, emission intensity in the absence of $O_2$) is indispensable for reliable quantification of $O_2$.[24,27,59] To avoid frequent calibrations, ratiometric $O_2$ detection based on phosphorescent ($O_2$ sensitive) and fluorescent ($O_2$ insensitive) dyes is a promising approach.[60–62] In the present study, ratiometric $O_2$ sensing was achieved simply by blending two types of liquids. Since both **PtPL** and **PyL** are hydrophobic and have similar liquid physical properties due to the same 2-hexyldecyl branched alkyl chains, the two liquids are miscible with each other,[63] and the blended liquid contains absorption profiles from both individual components (Fig. 5a and b). Two films (A and B) with different loadings were prepared from the blended liquid of **PtPL+PyL** (1 : 2, by weight) and investigated for ratiometric $O_2$ sensing (Fig. 5c). Upon excitation at 360 nm, the fluorescence ($\lambda_{em} = 428$ nm) from **PyL** is insensitive to $O_2$, while the phosphorescence from **PtPL** ($\lambda_{em} = 656$ nm) is sensitive to $O_2$. Stern–Volmer plots of the two films are highly linear ($R^2 > 0.999$), and the value of $I_0/I_{100}$ in film A reaches ~120 (comparable to that of **PtTPP–PTMSP** in Fig. 4d). A increase in $O_2$ sensitivity in the liquid blend system (compared with a neat liquid film of **PtPL**) may originate from enhanced $O_2$ solubility and/or diffusion in the liquid upon blending with the relatively smaller-sized molecule **PyL**. Stern–Volmer plots of films A and B are slightly different, presumably due to differences in the loading amount of liquid or experimental errors. Nevertheless, when ratios of phosphorescence and fluorescence are plotted against $O_2$ levels, films A and B demonstrate almost identical linear lines despite nearly double the difference in their emission intensity. Thus, the miscibility of liquids offers reliable ratiometric $O_2$ sensing without the need for elaborate synthesis, fine-tuning of film loading, and frequent calibrations.

To confirm the enhanced sensitivity in the blended system, the sensitivity ($I_0/I_{100}$) of six independently prepared **PtPL** and **PtPL+PyL** films was statistically analyzed (Tables S2 and S3). As a result, the average sensitivity of **PtPL+PyL** ($I_0/I_{100} = 113.2$, $\sigma = 3.3$) was reproducibly higher than that of **PtPL** ($I_0/I_{100} = 75.3$, $\sigma = 1.8$). The sensitivity of **PtPL** in Fig. 3d ($I_0/I_{100} \approx 90$) is slightly higher than that shown in Table S2 ($I_0/I_{100} = 75.3$ on average). This moderate difference can be attributed to cumulative decay of the emission intensity upon repeated exposure to excitation light (see Fig. 4f). The data in Fig. 3 were obtained at multiple $O_2$ levels, with 100% $O_2$ measured at the final stage of the experiment, which likely led to a reduction in the $I_{100}$ value compared to its actual value. In contrast, the data in Table S2 were obtained from only two measurements, namely under $N_2$ for $I_0$ and under $O_2$ for $I_{100}$. Therefore, the values reported in Table S2 are considered to be more reliable.

# Conclusions

This work reveals numerous benefits of luminescent core-isolated solvent-free liquids for optical gas sensing applications. Due to the liquid characteristics (*e.g.*, homogeneity, gas solubility, diffusion, and miscibility) and the shielding effects of the phosphorescent-core units by the bulky yet flexible alkyl chains, the Pt(II) porphyrin liquid demonstrates exceptional sensitivity, linearity, photostability, and calibration-free ratiometric operations in phosphorescent $O_2$ sensing. The concept presented in this study is broadly applicable to other functional π-chromophores and gaseous species, paving the way for a new platform for optical sensing materials.

# Methods

### Synthesis of PtPL

A previously reported liquid free-base porphyrin[13] was used to prepare a liquid Pt(II) porphyrin (**PtPL**). Typically, the alkylated free-base porphyrin (140 mg, 0.055 mmol) and Pt(II)$Cl_2$ (147 mg, 0.55 mmol) were refluxed in dry benzonitrile (15 ml) under an Ar atmosphere,[51] and the progress of metalation was monitored by thin-layer chromatography (TLC) and variation in the Q-bands in the UV-vis spectrum. After the reaction (*ca.* 4–5 h) was completed, the solvent was removed under reduced pressure, and the crude product was purified by column chromatography on silica gel (eluent: 10–20% $CH_2Cl_2$ in *n*-hexane). After drying under vacuum at 40 °C, a red-orange liquid (**PtPL**) was obtained (yield: 80%). $^1$H NMR (400 MHz, $CDCl_3$) in ppm: 8.86 (s, 8H, pyrrole β-H), 7.29 (d, $J = 2.4$ Hz, 8H, Ar–H), 6.86 (t, $J = 2.0$ Hz, 4H, Ar–H), 3.96 (d, $J = 5.6$ Hz, 16H, $OCH_2$), 1.83 (m, 8H, CH), 1.35–1.23 (m, 192H, $CH_2$), 0.82 (m, 48H, $CH_3$). $^{13}$C NMR (100 MHz, $CDCl_3$) in ppm: 158.68, 143.04, 140.62, 130.64, 122.18, 113.44, 101.21, 71.27, 38.10, 31.89, 31.86, 31.42, 30.03, 29.71, 29.59, 29.33, 26.87, 22.66, 14.11. HR-ESI-MS (*m*/*z*): calculated for $[C_{172}H_{285}O_8N_4{}^{194}Pt]^+ = 2729.1639$ *m*/*z*, found 2729.1736 *m*/*z*.

### Preparation of liquid films

Liquid films for $O_2$ sensing were obtained by spin-coating a toluene solution of liquid materials onto a quartz substrate. Typically, it took 5 seconds to reach 3000 rpm, and the film was dried at 3000 rpm for 60 seconds. Thus, homogeneous liquid films were obtained. The loading amount of the liquid film was adjusted by changing the concentration of the toluene solution or repeating the spin-coating process. A blended liquid film of **PtPL+PyL** was prepared from a solution of **PtPL** and **PyL** in toluene (1 : 2, by weight). Liquid films were dried in air for more than 12 h before spectroscopic measurements. See Fig. S20 for a discussion of residual solvent in a liquid film.

### Preparation of polymer films

Stock solutions of **PtPL** in dichloromethane (5.00 mg ml$^{-1}$) and **PTMSP**[49,64] in toluene (10.0 mg ml$^{-1}$) were mixed at various

ratios. The mixed solutions were spin-coated on a quartz substrate, as described above. In the case of **PtTPP**, a more diluted stock solution (1.67 mg $ml^{-1}$) in dichloromethane was used due to limited solubility. See Fig. S19 for a discussion on the homogeneity of **PtPL** in polymer films.

### $O_2$ sensing

The porphyrin film containing quartz substrate was placed in a quartz cell (1 cm × 1 cm), as illustrated in Fig. S1. The quartz cell was capped with a rubber septum, and then dry $N_2$ or Ar containing various concentrations of $O_2$ was flowed through the cell using inlet and outlet needles to measure emission spectra (FP-8300 spectrophotometer, JASCO) under controlled $O_2$ levels. The typical flow rate was 100 ml $min^{-1}$, and 5 min flow was sufficient to replace the interior gases of the small cell (~3 ml). The flow rate was adjusted and monitored using a float-ball-type flow meter (KOFLOCK) and a digital flow meter (7000 flow-meter, Ellutia). Dry $N_2$ and $O_2$ from laboratory lines were used as 0% and 100% $O_2$, respectively. Ambient air supplied by a battery-powered pump (GSP-400FT, GASTEC) was regarded as 21% $O_2$. For 0.1%, 1%, and 10% $O_2$, standard gases supplied from high-pressure gas cylinders were directly used. For 50% and 80% $O_2$, dry $N_2$ and $O_2$ from laboratory lines were mixed at appropriate flow rates (monitored by digital flow meters). Similarly, 0.1% $O_2$ with dry $N_2$ dilution yielded 0.03% $O_2$.

## Author contributions

A. G. and T. M. synthesized porphyrins. A. G., S. I., and T. M. performed sensing experiments. M. K. C. and D. T. P. conducted material characterization. A. S. measured transient emission properties. T. H. provided PTMSP and discussed the results of $O_2$ sensing. S. I. wrote the manuscript with input from all other authors. All authors read and approved the final version of the manuscript. S. I. and T. N. designed and directed the research.

## Conflicts of interest

The authors declare no conflicts of interest.

## Note added after first publication

This version replaces the manuscript published on 22nd January 2026 which contained an error in the caption for Fig. 4d. **PtPL** should have been **PtTPP–PTMSP**. The RSC apologises for any confusion.

## Data availability

The data presented in this study are available upon reasonable request from the corresponding authors. Supplementary information (SI) is available for materials, methods, characterizations, photophysical and statistical analyses, and miscellaneous data. See DOI: https://doi.org/10.1039/d5sc08398b.

## Acknowledgements

This work was supported by JSPS KAKENHI (JP18H03922, JP24H01733, JP25H01264). This work was supported by the World Premier International Research Center Initiative (WPI), MEXT, Japan. Ms. Reiko Takano is acknowledged for assisting with sensing measurements. Dr Zhenfeng Guo and Mr Mina Fahmy are acknowledged for supporting the spectroscopic measurements.

## References

1 *Functional Organic Liquids*, ed. T. Nakanishi, Wiley-VCH, Weinheim 2019.
2 A. Ghosh and T. Nakanishi, Frontiers of Solvent-Free Functional Molecular Liquids, *Chem. Commun.*, 2017, **53**, 10344–10357.
3 F. Lu and T. Nakanishi, Solvent-Free Luminous Molecular Liquids, *Adv. Opt. Mater.*, 2019, **7**, 1900176.
4 A. Tateyama and T. Nakanishi, Responsive Molecular Liquid Materials, *Responsive Mater.*, 2023, **1**, e20230001.
5 S. S. Babu, J. Aimi, H. Ozawa, N. Shirahata, A. Saeki, S. Seki, A. Ajayaghosh, H. Möhwald and T. Nakanishi, Solvent-Free Luminescent Organic Liquids, *Angew. Chem., Int. Ed.*, 2012, **51**, 3391–3395.
6 A. M. Goudappagouda, V. C. Wakchaure, K. C. Ranjeesh, T. Das, K. Vanka, T. Nakanishi and S. S. Babu, Paintable Room-Temperature Phosphorescent Liquid Formulations of Alkylated Bromonaphthalimide, *Angew. Chem., Int. Ed.*, 2019, **58**, 2284–2288.
7 M. Komura, T. Ogawa and Y. Tani, Room-Temperature Phosphorescence of a Supercooled Liquid: Kinetic Stabilisation by Desymmetrisation, *Chem. Sci.*, 2021, **12**, 14363–14368.
8 A. Ikenaga, Y. Akiyama, T. Ishiyama, M. Gon, K. Tanaka, Y. Chujo and K. Isoda, Stimuli-Responsive Self-Assembly of π-Conjugated Liquids Triggers Circularly Polarized Luminescence, *ACS Appl. Mater. Interfaces*, 2021, **13**, 47127–47133.
9 Y. Tani, Y. Oshima, R. Okada, J. Fujimura, Y. Miyazaki, M. Nakano, O. Urakawa, T. Inoue, T. Ehara, K. Miyata, K. Onda and T. Ogawa, Fast and Efficient Room-Temperature Phosphorescence from Metal-Free Organic Molecular Liquids, *Chem. Sci.*, 2025, **16**, 17480–17486.
10 P. Duan, N. Yanai and N. Kimizuka, Photon Upconverting Liquids: Matrix-Free Molecular Upconversion Systems Functioning in Air, *J. Am. Chem. Soc.*, 2013, **135**, 19056–19059.
11 R. K. Gupta, T. Nakanishi and D. T. Payne, Alkyl-π Liquids as Condensed-State Singlet Oxygen Photosensitizers, *Chem. – Eur. J.*, 2025, **31**, e202500739.
12 S. Hirata, K. Kubota, H. H. Jung, O. Hirata, K. Goushi, M. Yahiro and C. Adachi, Improvement of Electroluminescence Performance of Organic Light-Emitting Diodes with a Liquid-Emitting Layer by Introduction of Electrolyte and a Hole-Blocking Layer, *Adv. Mater.*, 2011, **23**, 889–893.

13 A. Ghosh, M. Yoshida, K. Suemori, H. Isago, N. Kobayashi, Y. Mizutani, Y. Kurashige, I. Kawamura, M. Nirei, O. Yamamuro, T. Takaya, K. Iwata, A. Saeki, K. Nagura, S. Ishihara and T. Nakanishi, Soft Chromophore Featured Liquid Porphyrins and their Utilization toward Liquid Electret Applications, *Nat. Commun.*, 2019, **10**, 4210.

14 Y. Shi, M. A. Gerkman, Q. Qiu, S. Zhang and G. D. D. Han, Sunlight-Activated Phase Change Materials for Controlled Heat Storage and Triggered Release, *J. Mater. Chem. A*, 2021, **9**, 9798–9808.

15 N. Giri, M. G. Del Pópolo, G. Melaugh, R. L. Greenaway, K. Rätzke, T. Koschine, L. Pison, M. F. Costa Gomes, A. I. Cooper and S. L. James, Liquids with Permanent Porosity, *Nature*, 2015, **527**, 216–220.

16 Y.-H. Zou, Y.-B. Huang, D.-H. Si, Q. Yin, Q.-J. Wu, Z. Weng and R. Cao, Porous Metal–Organic Framework Liquids for Enhanced $CO_2$ Adsorption and Catalytic Conversion, *Angew. Chem., Int. Ed.*, 2021, **60**, 20915–20920.

17 M. J. Hollamby, M. Karny, P. H. H. Bomans, N. A. J. M. Sommerdjik, A. Saeki, S. Seki, H. Minamikawa, I. Grillo, B. R. Pauw, P. Brown, J. Eastoe, H. Möhwald and T. Nakanishi, Directed Assembly of Optoelectronically Active Alkyl-π-Conjugated Molecules by Adding n-Alkanes or π-Conjugated Species, *Nat. Chem.*, 2014, **6**, 690–696.

18 T. Ogoshi, K. Maruyama, Y. Sakatsume, T. Kakuta, T. Yamagishi, T. Ichikawa and M. Mizuno, Guest Vapor-Induced State Change of Structural Liquid Pillar[6]arene, *J. Am. Chem. Soc.*, 2019, **141**, 785–789.

19 A. Shinohara, C. Pan, Z. Guo, L. Zhou, Z. Liu, L. Du, Z. Yan, F. J. Stadler, L. Wang and T. Nakanishi, Viscoelastic Conjugated Polymer Fluids, *Angew. Chem., Int. Ed.*, 2019, **58**, 9581–9585.

20 K. Isoda, M. Matsubara, A. Ikenaga, Y. Akiyama and Y. Mutoh, Reversibly/Irreversibly Stimuli-Responsive Inks Based on N-Heteroacene Liquids, *J. Mater. Chem. C*, 2019, **7**, 14075–14079.

21 K. Isoda, T. Ishiyama, Y. Mutoh and D. Matsukuma, Stimuli-Responsive Room-Temperature *N*-Heteroacene Liquid: *In Situ* Observation of the Self-Assembling Process and Its Multiple Properties, *ACS Appl. Mater. Interfaces*, 2019, **11**, 12053–12062.

22 *'Henry's law' in IUPAC Compendium of Chemical Terminology*, edn. 5th edn, International Union of Pure and Applied Chemistry, 2025, Online version 5.0.0, 2025, DOI: 10.1351/goldbook.H02783.

23 O. S. Wolfbeis, Materials for Fluorescence-Based Optical Chemical Sensors, *J. Mater. Chem.*, 2005, **15**, 2657–2669.

24 C. McDonagh, C. S. Burke and B. D. MacCraith, Optical Chemical Sensors, *Chem. Rev.*, 2008, **108**, 400–422.

25 S. W. Thomas, G. D. Joly and T. M. Swager, Chemical Sensors Based on Amplifying Fluorescent Conjugated Polymers, *Chem. Rev.*, 2007, **107**, 1339–1386.

26 J. Kramer, R. Kang, L. M. Grimm, L. De Cola, P. Picchetti and F. Biedermann, Molecular Probes, Chemosensors, and Nanosensors for Optical Detection of Biorelevant Molecules and Ions in Aqueous Media and Biofluids, *Chem. Rev.*, 2022, **122**, 3459–3636.

27 X.-D. Wang and O. S. Wolfbeis, Optical Methods for Sensing and Imaging Oxygen: Materials, Spectroscopies and Applications, *Chem. Soc. Rev.*, 2014, **43**, 3666–3761.

28 R. Ramamoorthy, P. K. Dutta and S. A. Akbar, Oxygen Sensors: Materials, Methods, Designs and Applications, *J. Mater. Sci.*, 2003, **38**, 4271–4282.

29 A. A. Mendonsa and K. J. Cash, Oxygen-Sensitive Optical Nanosensors: Current Advances and Future Perspectives, *ACS Sens.*, 2025, **10**, 3194–3206.

30 J. W. Gregory, H. Sakaue, T. Liu and J. P. Sullivan, Fast Pressure-Sensitive Paint for Flow and Acoustic Diagnostics, *Annu. Rev. Fluid. Mech.*, 2014, **46**, 303–330.

31 J. Inukai, K. Miyatake, K. Takada, M. Watanabe, T. Hyakutake, H. Nishide, Y. Nagumo, M. Watanabe, M. Aoki and H. Takano, Direct Visualization of Oxygen Distribution in Operating Fuel Cells, *Angew. Chem., Int. Ed.*, 2008, **47**, 2792–2795.

32 Y. E. Koo Lee, E. E. Ulbrich, G. Kim, H. Hah, C. Strollo, W. Fan, R. Gurjar, S. Koo and R. Kopelman, Near Infrared Luminescent Oxygen Nanosensors with Nanoparticle Matrix Tailored Sensitivity, *Anal. Chem.*, 2010, **82**, 8446–8455.

33 X. Zheng, H. Mao, D. Huo, W. Wu, B. Liu and X. Jiang, Successively Activatable Ultrasensitive Probe for Imaging Tumour Acidity and Hypoxia, *Nat. Biomed. Eng.*, 2017, **1**, 0057.

34 J. Mei, N. L. C. Leung, R. T. K. Kwok, J. W. Y. Lam and B. Z. Tang, Aggregation-Induced Emission: Together We Shine, United We Soar, *Chem. Rev.*, 2015, **115**, 11718–11940.

35 Y. Amao, Probes and Polymers for Optical Sensing of Oxygen, *Microchim. Acta*, 2003, **143**, 1–12.

36 S. M. Borisov, A. S. Vasylevska, C. Krause and O. S. Wolfbeis, Composite Luminescent Material for Dual Sensing of Oxygen and Temperature, *Adv. Funct. Mater.*, 2006, **16**, 1536–1542.

37 H. Xiang, L. Zhou, Y. Feng, J. Cheng, D. Wu and X. Zhou, Tunable Fluorescent/Phosphorescent Platinum(II) Porphyrin–Fluorene Copolymers for Ratiometric Dual Emissive Oxygen Sensing, *Inorg. Chem.*, 2012, **51**, 5208–5212.

38 S.-K. Lee and I. Okura, Porphyrin-Doped Sol-Gel Glass as a Probe for Oxygen Sensing, *Anal. Chim. Acta*, 1997, **342**, 181–188.

39 S. M. Borisov, P. Lehner and I. Klimant, Novel Optical Trace Oxygen Sensors Based on Platinum(II) and Palladium(II) Complexes with 5,10,15,20-meso-Tetrakis-(2,3,4,5,6-pentafluorphenyl)-porphyrin Covalently Immobilized on Silica-Gel Particles, *Anal. Chim. Acta*, 2011, **690**, 108–115.

40 C.-S. Chu and Y.-L. Lo, High-Performance Fiber-Optic Oxygen Sensors Based on Fluorinated Xerogels Doped with Pt(II) Complexes, *Sens. Actuators, B*, 2007, **124**, 376–382.

41 B.-H. Han, I. Manners and M. A. Winnik, Oxygen Sensors Based on Mesoporous Silica Particles on Layer-by-Layer Self-Assembled Films, *Chem. Mater.*, 2005, **17**, 3160–3171.

42 T. Burger, C. Winkler, I. Dalfen, C. Slugovc and S. M. Borisov, Porphyrin Based Metal–Organic Frameworks: Highly Sensitive Materials for Optical Sensing of Oxygen in Gas Phase, *J. Mater. Chem. C*, 2021, **9**, 17099–17112.

43 Y. E. Koo, Y. Cao, R. Kopelman, S. M. Koo, M. Brasuel and M. A. Philbert, Real-Time Measurements of Dissolved Oxygen Inside Live Cells by Organically Modified Silicate Fluorescent Nanosensors, *Anal. Chem.*, 2004, **76**, 2498–2505.

44 X.-D. Wang, J. A. Stolwijk, T. Lang, M. Sperber, R. J. Meier, J. Wegener and O. S. Wolfbeis, Ultra-Small, Highly Stable, and Sensitive Dual Nanosensors for Imaging Intracellular Oxygen and pH in Cytosol, *J. Am. Chem. Soc.*, 2012, **134**, 17011–17014.

45 C. M. Lemon, E. Karnas, M. G. Bawendi and D. G. Nocera, Two-Photon Oxygen Sensing with Quantum Dot-Porphyrin Conjugates, *Inorg. Chem.*, 2013, **52**, 10394–10406.

46 Y. Amao and I. Okura, Optical Oxygen Sensor Devices Using Metalloporphyrins, *J. Porphyrins Phthalocyanines*, 2009, **13**, 1111–1122.

47 I. Okura and T. Kamachi, Applications of Porphyrins and Related Compounds as Optical Oxygen Sensors, in *Handbook of Porphyrin Science*, ed. K. M. Kadish, K. M. Smith and R. Guilard, World Scientific Publishing, Singapore, 2011, vol. 12, pp. 297–348.

48 S. Ishihara, J. Labuta, W. V. Rossom, D. Ishikawa, K. Minami, J. P. Hill and K. Ariga, Porphyrin-Based Sensor Nanoarchitectonics in Diverse Physical Detection Modes, *Phys. Chem. Chem. Phys.*, 2014, **16**, 9713–9746.

49 T. Masuda, E. Isobe, T. Higashimura and K. Takada, Poly[1-(trimethylsilyl)-1-propyne]: A New High Polymer Synthesized with Transition-Metal Catalysts and Characterized by Extremely High Gas Permeability, *J. Am. Chem. Soc.*, 1983, **105**, 7473–7474.

50 Y. Amao, K. Asai, I. Okura, H. Shinohara and H. Nishide, Platinum Porphyrin Embedded in Poly(1-trimethylsilyl-1-propyne) Film as an Optical Sensor for Trace Analysis of Oxygen, *Analyst*, 2000, **125**, 1911–1914.

51 W. Wu, W. Wu, S. Ji, H. Guo, X. Wang and J. Zhao, The Synthesis of 5, 10, 15, 20-Tetraarylporphyrins and their Platinum (II) Complexes as Luminescent Oxygen Sensing Materials, *Dyes Pigm.*, 2011, **89**, 199–211.

52 A. Gugliuzza, A. Iulianelli and A. Basile, Membranes for Hydrocarbon Fuel Processing and Separation, in *Advanced Membrane Science and Technology for Sustainable Energy and Environmental Applications*, Elsevier, 2011, pp. 295–338.

53 E. R. Carraway, J. N. Demas, B. A. DeGraff and J. R. Bacon, Photophysics and Photochemistry of Oxygen Sensors Based on Luminescent Transition-Metal Complexes, *Anal. Chem.*, 1991, **63**, 337–342.

54 J. N. Demas, B. A. DeGraff and W. Xu, Modeling of Luminescence Quenching-Based Sensors: Comparison of Multisite and Nonlinear Gas Solubility Models, *Anal. Chem.*, 1995, **67**, 1377–1380.

55 P. Hartmann, M. J. P. Leiner and M. E. Lippitsch, Luminescence Quenching Behavior of an Oxygen Sensor Based on a Ru(II) Complex Dissolved in Polystyrene, *Anal. Chem.*, 1995, **67**, 88–93.

56 W. Xu, R. C. McDonough, B. Langsdorf, J. N. Demas and B. A. DeGraff, Oxygen Sensors Based on Luminescence Quenching: Interactions of Metal Complexes with the Polymer Supports, *Anal. Chem.*, 1994, **66**, 4133–4141.

57 W. W. S. Lee, K. Y. Wong, X. M. Li, Y. B. Leung, C. S. Chan and K. S. Chan, Halogenated Platinum Porphyrins as Sensing Materials for Luminescence-Based Oxygen Sensors, *J. Mater. Chem.*, 1993, **3**, 1031–1035.

58 F. Lu, T. Takaya, K. Iwata, I. Kawamura, A. Saeki, M. Ishii, K. Nagura and T. Nakanishi, A Guide to Design Functional Molecular Liquids with Tailorable Properties using Pyrene-Fluorescence as a Probe, *Sci. Rep.*, 2017, **7**, 3416.

59 P. Lehner, C. Staudinger, S. M. Borisov, J. Regensburger and I. Klimant, Intrinsic Artifacts in Optical Oxygen Sensors—How Reliable are our Measurements?, *Chem. – Eur. J.*, 2015, **21**, 3978–3986.

60 Y. Feng, J. Cheng, L. Zhou, X. Zhou and H. Xiang, Ratiometric Optical Oxygen Sensing: A Review in Respect of Material Design, *Analyst*, 2012, **137**, 4885–4901.

61 T. Hyakutake, I. Okura, K. Asai and H. Nishide, Dual-Mode Oxygen-Sensing Based on Oxygen-Adduct Formation at Cobaltporphyrin–Polymer and Luminescence Quenching of Pyrene: An Optical Oxygen Sensor for a Practical Atmospheric Pressure, *J. Mater. Chem.*, 2008, **18**, 917–922.

62 H. Zhao, L. Zang, L. Wang, F. Qin, Z. Zhang and W. Cao, Luminescence Ratiometric Oxygen Sensor Based on Gadolinium Labeled Porphyrin and Filter Paper, *Sens. Actuators, B*, 2015, **215**, 405–411.

63 Z. Guo, C. Pan, A. Shinohara and T. Nakanishi, Merging π-Molecular Functions Achieved through Homogeneous Liquid-Liquid Blending of Solvent-Free Alkyl-π Liquids, *Sci. Technol. Adv. Mater.*, 2025, **26**, 2515007.

64 W. Waskitoaji, T. Hyakutake, J. Kato, M. Watanabe and H. Nishide, Biplanar Visualization of Oxygen Pressure by Sensory Coatings of Luminescent Pt-Porpholactone and -Porphyrin Polymers, *Chem. Lett.*, 2009, **38**, 1164–1165.